する指針が定められているが、脳神経倫理に関してはまだ専門的倫理指針がないのが実情であり、BMI研究の進展を考慮すると早急に検討を行うべき時期にあると思われる。

こうした倫理指針を制定するにあたってはしっかりとした学問的基盤が必須となるが、学問的には精神、意識、自我の主座である脳という臓器の特殊性・重要性を考慮すると、独立した学問領域として扱うべき面がある一方で、エンハンスメントなど遺伝子・幹細胞等他の研究分野と共通した問題点については、共通化して応用倫理として包括的に扱うべき側面も指摘されている[19]。これらの動きは、実用的には必要十分な倫理規範体系を構築し、むやみに多くの倫理指針を制定して、逆に遵守することが煩雑になるのを防ぐのにも貢献するものと期待される。

BMIと脳神経倫理

本邦ではBMI研究の気運が高まるとともに脳神経倫理に注目が集まったが、その第一の理由は脳情報流出の問題があろう。BMIのキーとなる基盤技術としてニューラルデコーディングと呼ばれる技術があり、これは脳信号からその人の脳活動の内容を読み取ることを可能にする。例えば筆者らは、難治性のてんかんや難治性の疼痛の治療目的で脳表面に電極を留置した患者さんの協力を得て、脳表脳波を用いた脳機能再建の研究を行い、そのひとの手の動きを、数種類であれば80-90%の精度で推定することに成功し[20]、現在、実用的には初歩的なレベルではあるが、ロボットアームをリアルタイムに制御できるレベルにある[21,22]。またATR脳情報研究所の神谷らはfMRIの信号から被験者が見ている文字を再構成することに成功している[23]。これらの脳活動読み取りは運動や視覚に限られており、脳機能の精神や感情的な領域にまでは踏み込んではいない。しかし、こうした技術が進歩すると、精神や感情の領域に踏み込む可能性も考えられ、マインドリーディングが実現することになる。ある種の精神や感情を内に秘めて、外部に出したくないのは人間にとっていわば当たり前のことであり、これが守られないとなると倫理的問題が大きいというのも自明の理であろう。そのため、ニューラルデコーデ

ィング技術が進歩してマインドリーディングが実現する前に、十分な倫理的検討と対策を行う必要が生じてくる。狭義のBMIは脳信号を計測して、読み取り結果にもとづいて外部機器を制御するだけなので、脳刺激療法等に比較して脳への影響の問題は少ないと思われる。しかしその長期的影響は明らかでなく、長期間の利用により予期せぬ脳機能変容の可能性がある。Denningらは、神経デバイスにより脳情報が流出する危険性を指摘し、Neurosecurityという言葉を定義して、脳情報流出に対する機器のセキュリティの重要性を訴えている(24)。

染谷らは脳情報が果たして究極のプライバシーかどうかという問題に関して検討している。彼らによれば、心のプライバシーの内実も、心もしくは脳が備えている本質的に例外的な特質によってではなく、脳情報を利用しようとする社会的・経済的な運動によって与えられているという。例えば、マインドリーディング技術から得られる情報を、医療目的の他に、企業の広告宣伝活動、雇用や保険の契約判断、犯罪捜査上の手がかりといった目的のために利用する社会の側からの要請が、脳情報を特別な価値を持つものとして脚色し、プライバシー性を高める。究極にしているのは心や脳そのものではなく、脳研究の結果を利用しようとする社会である。そして、こうした脳情報に関する誤用や乱用を避けるためには、暫定的処置として利用範囲や利用目的を規制する法的保護と、実質的な処置として脳神経科学に対する大衆の理解向上に努めることが重要であると述べている(2)。エンハンスメントや軍事応用には具体的な言及はしていないが、染谷らの主張はこれらの社会的要請にもあてはめることができよう。

BMIに関連する医療技術として深部脳刺激療法（Deep Brain Stimulation: DBS）という治療法がある。これは基底核と呼ばれる大脳の深部構造に電極を刺入し、電気刺激するとパーキンソン病などの難治性の不随意運動疾患が劇的に緩和されることから、近年本邦でも着実に普及している治療法である。このDBSは、欧米では精神疾患の外科治療を目指して、近年、臨床研究が盛んに行われている。しかし、1930～1950年代に盛んに行われた、ロボトミーをはじめとする精神疾患の外科的治療の弊害が明らかになり、日本精神神

経学会が1975年に精神外科を否定する決議を採択するなど、精神疾患に対する外科的治療に対して否定的見解が強い。

臨床研究に対して、現状の医学水準のみを考慮して画一的に判断したり、印象や感情的な要素に流されて危険性を過大評価することも、医学の進歩を妨げ、より良い医療を将来提供する機会を奪うことにつながりかねない。特に、本邦の国民感情や報道の特殊性に関しては留意する必要がある。例えば、精神操作は薬物治療ではすでにいろいろな治療が行われているとも言え、その中には少なからぬ副作用を示すものがあるのも事実であるが、外科治療となればそれだけで批判的評価を多くの人が下すのではないかと危惧する意見もある(25)。報道に関しては、海外での研究的治療はあたかも標準的治療であるかのように報道する風潮があることが指摘されている(25)。また、本邦では外科的治療に際して家族の意見も考慮される傾向が強いとの指摘もある(26)。こうした我が国の事情を踏まえて、欧米を中心とした新しい精神外科治療の臨床試験の状況を高木らを中心としたグループが調査した。その結果を踏まえて、高木らは「脳神経疾患に限らず、臨床研究の審査にあたっては、有効性と安全性・倫理性を正しく評価して比較検討する必要があるが、そもそも定量比較が困難なものも多く、絶対的正解のない作業であることを覚悟の上で、各種委員会はある一線を引かなくてはならない」と提言している(26)。

脳神経倫理への個別対応と包括的対応

前述したように、現時点では脳神経倫理に関する公的な指針や法的規制は定められていないが、BMIの医療応用に対する患者の期待は大きく、一般の人々に関しても医療応用に対しては肯定的意見が多数を占める。筆者らは全国のALS患者約2000名を対象にしてBMIに関するアンケート調査を実施したところ、約8割の患者がBMIに関心を示した。また福山らはインターネット上で2500名の一般の人々にアンケート調査を行ったところ、BMIの医療応用には約8割の人が賛成した。こうしたことから、大まかな方針としては、倫理的な問題点に十分な検討と対策を行った上で、医療応用の実用化を図るのが最も妥当な選択と思われる。筆者らは臨床研究者として、こうした方針

にもとづいて倫理的問題に対応しながら、基礎的な研究開発から臨床研究を行って、BMIの医療応用を目指している(6)。

筆者らが参加している文部科学省脳科学研究戦略推進プログラムでは、倫理相談窓口を設置してプロジェクト内の倫理的課題に対して対応している。実際、個々のBMIの臨床研究の倫理審査においては、神経倫理の専門家がいまだ少ないため、施設内倫理委員会だけでは神経倫理学的な事項に関して必ずしも十分な審査体制にあるとは限らない。そこで倫理相談窓口を活用して、あらかじめ神経倫理学的問題点に対して対応をしておくことが重要である。

筆者らは平成23年9月までにBMI関係で9件の倫理審査を病院倫理審査委員会に申請しているが、プロジェクト内に倫理相談窓口が設置された後に申請した6件のうち5件を倫理相談窓口に事前に提出し、神経倫理学的な課題の抽出や対策を行っている。その内訳は、患者アンケート調査3件、P300スペラーによるBMI、重症ALS患者を対象としたBMI臨床研究である。

個々のBMIの臨床研究に対する個別的な倫理対応に加えて、より包括的な倫理への対応も行われている。BMIの医療応用を早期に実現するために、筆者らは厚生労働省が行う次世代医療機器評価指標作成事業に参加し、BMIのガイドラインを作成した。その中で、臨床試験の安全性の評価に関して、脳の可塑性にもとづく予期せぬ脳活動の変調、およびそれに伴う副作用の有無、個人の脳活動が外部に出力されることに起因する個人情報への影響や不利益などの神経倫理学的な問題の評価を行うよう記載している(27)。

学会活動に関しては、日本神経科学会の学術大会である日本神経科学大会では2009年以降、毎年神経倫理のセッションがシンポジウムとして開催されており、重要課題として認識されている。また、日本定位機能神経外科学会では2010年の大阪大学主催の大会にて「ニューロモデュレーションと神経倫理」というテーマで神経倫理のシンポジウムを企画し、東京大学情報学環の佐倉統教授が、「先端医療と一般社会―2つの文化の隙間を、新しい技術が進む―」というタイトルで発表を行ったほか、DBSによる精神疾患治療に関する倫理的問題、埋込BMI装置に関する問題などが議論された。

筆者とともに文部科学省脳科学研究戦略推進プログラムにおいてBMIの研

究開発に取り組む川人（研究代表者）や佐倉（脳神経倫理担当）らは、BMIに関する重要な倫理として、以下に挙げるBMI倫理4原則を提案している[28]。

原則1：戦争や犯罪にBMIを利用してはならない。

原則2：何人も本人の意思に反してBMI技術で心を読まれてはならない。

原則3：何人も本人の意思に反してBMI技術で心を制御されてはならない。

原則4：BMI技術は、その効用が危険とコストを上回り、それを使用者が確認するときのみ利用されるべきである。

これは1950年にアイザックアシモフが自身の著書『われはロボット』のなかで、提案したロボット工学3原則[29]を参考にして考案したもので、BMIに要求される倫理を簡潔に示したものと言える。今後はこれを踏まえた脳神経倫理指針の策定が望まれるところである。

脳神経疾患に限らず、臨床研究の審査にあたっては、有効性と安全性・倫理性を正しく評価して比較検討する必要があるが、そもそも定量比較が困難なものも多く、絶対的正解のない作業であることを覚悟の上で、各種委員会はある一線を引かなくてはならない、とDBSを用いた精神疾患治療に関する倫理的考察のなかで高木らは述べている[26]。これはBMIにもそのまま適用できる。こうした作業を経て、有効性、安全性、倫理性をその時点でできうる最高のレベルまで高める検討と対策を事前に行ったうえで、臨床研究を遅滞なく進め、最終的にはより良い医療を提供する姿勢が臨床研究者にとって

（参考）

ロボット工学3原則

第1条：ロボットは人間に危害を加えてはならない。また、その危機を看過することによって、人間に危害を与えてはならない。

第2条：ロボットは人間に与えられた命令に服従しなければならない。ただし与えられた命令が第一条に反する場合は、この限りではない。

第3条：ロボットは前掲第一条および第二条に反するおそれのないかぎり、自己を守らねばならない。

は肝要と言えよう。

謝辞

筆者らは文部科学省の脳科学研究戦略推進プログラムの研究助成を受けており、課題の代表研究者 ATR 脳情報研究所の川人光男先生、機関代表研究者の大阪大学脳神経外科の吉峰俊樹先生に感謝致します。本稿の執筆にあたっては同プログラムの東京大学情報学環の佐倉統先生、水島希先生には貴重なご助言を頂きました。ここに深謝いたします。

〔引用文献〕

(1) 平田雅之，吉峰俊樹．Brain-Machine Interface. Clinical Neuroscience. 2011；29(6)：384-7.
(2) 染谷昌義，小口峰樹．「究極のプライバシー」が脅かされる!?　In：信原幸弘，原塑，editors. 脳神経倫理学の展望．勁草書房，2008.
(3) ジェームズ D. モレノ．操作される脳．アスキーメディアワークス，2008.
(4) 上田昌文，渡部麻衣子．エンハンスメント論争　身体・精神の増強と先端科学技術．社会評論社，2008.
(5) 美馬達哉．脳科学が社会に及ぼす影響．Brain and Nerve. 2009；61(1)：18-26.
(6) 平田雅之，吉峰俊樹．脳神経外科における BMI の展望．脳神経外科速報．2011；21(8)：880-9.
(7) 香川知晶．「応用倫理学」とモンスターの哲学．In：信原幸弘，塑原，editors. 脳神経倫理学の展望．勁草書房，2008. p.15-38.
(8) 福士珠美，佐倉統．日本の脳神経科学研究における倫理―現状と将来展望．Brain and Nerve. 2009；61(1)：5-10.
(9) マイクル S. ガザニカ．脳のなかの倫理．紀伊國屋書店，2006.
(10) 世界医師会，日本医師会訳．ヘルシンキ宣言　ヒトを対象とした臨床研究における倫理．Available from: http://www.med.or.jp/wma/helsinki08_j.html.
(11) 厚生労働省．臨床研究に関する倫理指針（平成 20 年厚生労働省告示第 415 号）．Available from: http://www.mhlw.go.jp/general/seido/kousei/i-kenkyu/#4.
(12) 文部科学省，厚生労働省．疫学研究に関する倫理指針（平成 20 年 12 月 1 日一部改正）．Available from: http://www.mhlw.go.jp/general/seido/kousei/i-kenkyu/ekigaku/0504sisin.html.
(13) 文部科学省，厚生労働省，経済産業省．ヒトゲノム・遺伝子解析研究に関する倫理指針（平成20年12月1日一部改正）．Available from: http://www.mhlw.go.jp/general/seido/kousei/i-kenkyu/genome/0504sisin.html.

(14) 文部科学省，厚生労働省．遺伝子治療臨床研究に関する指針（平成20年12月1日一部改正）．Available from: http://www.mhlw.go.jp/general/seido/kousei/i-kenkyu/idenshi/0504sisin.html.
(15) 厚生労働省，ヒト幹細胞を用いる臨床研究に関する指針（平成22年厚生労働省告示第380号）．Available from: http://www.mhlw.go.jp/bunya/kenkou/iryousaisei.html.
(16) 大阪大学．大阪大学研究倫理審査委員会規程．Available from: http://www.osaka-u.ac.jp/ja/research/iinkai/moral.
(17) 大阪大学医学部．大阪大学医学部医学倫理委員会規程．Available from: http://www.med.osaka-u.ac.jp/jpn/guide/committee/igaku_rinri.html.
(18) 大阪大学医学部附属病院．大阪大学医学部附属病院臨床研究倫理審査委員会規則．Available from: http://www.med.osaka-u.ac.jp/pub/hp-crc/person_concerned/clinical_study.html.
(19) 香川知晶．脳神経倫理と生命倫理—生命倫理のバルカン化論争と応用倫理の収斂．Brain and Nerve. 2009；61(1)：11-7.
(20) Yanagisawa T, Hirata M, Saitoh Y, Kato A, Shibuya D, Kamitani Y, et al. Neural decoding using gyral and intrasulcal electrocorticograms. Neuroimage. 2009 May 1；45(4)：1099-106.
(21) Yanagisawa T, Hirata M, Saitoh Y, Kishima H, Matsushita K, Goto T, et al. Electrocorticographic control of a prosthetic arm in paralyzed patients. Ann Neurol. in press.
(22) Yanagisawa T, Hirata M, Saitoh Y, Goto T, Kishima H, Fukuma R, et al. Real-time control of a prosthetic hand using human electrocorticography signals. J Neurosurg. 2011 Jun；114(6)：1715-22.
(23) Miyawaki Y, Uchida H, Yamashita O, Sato MA, Morito Y, Tanabe HC, et al. Visual image reconstruction from human brain activity using a combination of multiscale local image decoders. Neuron. 2008 Dec 10；60(5)：915-29.
(24) Denning T, Matsuoka Y, Kohno T. Neurosecurity：security and privacy for neural devices. Neurosurg Focus. 2009 Jul；27(1)：E7.
(25) 片山容一，深谷親．脳深部刺激療法をめぐる脳神経倫理．Brain and Nerve. 2009；61(1)：33-40.
(26) 高木美也子．脳深部刺激療法の精神疾患への適用に対する安全性と神経倫理的考察．Brain and Nerve. 2009；61(1)：33-40.
(27) 厚生労働省医薬食品局・医療機器審査管理室．次世代医療機器評価指標の公表について（平成22年12月15日薬食機発1215第1号）．2010；Available from: http://www.hourei.mhlw.go.jp/hourei/new/tsuchi/new.html.
(28) 川人光男，佐倉統．ブレイン・マシン・インターフェース　BMI倫理4原則の提案．現代化学．2010；471(6)：21-5.
(29) アイザックアシモフ．われはロボット．早川書房，1963.

Brain-Machine Interface Using Brain Surface Electrodes: Real-Time Robotic Control and a Fully Implantable Wireless System

Masayuki Hirata[1], Takufumi Yanagisawa[1], Kojiro Matsushita[1], Hisato Sugata[1], Yukiyasu Kamitani[2], Takafumi Suzuki[3], Hiroshi Yokoi[4], Tetsu Goto[1], Morris Shayne[1], Yoichi Saitoh[1], Haruhiko Kishima[1], Mitsuo Kawato[2], and Toshiki Yoshimine[1]

[1] *Department of Neurosurgery, Osaka University Medical School, Japan*

[2] *ATR Computational Neuroscience Laboratories, Japan*

[3] *Graduate School of Information Science and Technology, The University of Tokyo, Japan*

[4] *The University of Tokyo, Interfaculty Initiative in Information Studies, Japan*

ABSTRACT

The brain-machine interface (BMI) enables us to control machines and to communicate with others, not with the use of input devices, but through the direct use of brain signals. This paper describes the integrative approach we used to develop a BMI system with brain surface electrodes for real-time robotic arm control in severely disabled people, such as amyotrophic lateral sclerosis patients. This integrative BMI approach includes effective brain signal recording, accurate neural decoding, robust robotic control, a wireless and fully implantable device, and a noninvasive evaluation of surgical indications.

INTRODUCTION

The **brain-machine interface** (**BMI**) is a man-machine interface that enables us to control machines and to communicate with others not with the use of input devices, but through the direct use of brain signals alone (Figure 1). Several diseases and conditions can lead to the loss of muscular control without a disruption in patients' brain function, including amyotrophic lateral sclerosis (ALS), brainstem stroke, spinal cord injury, and muscular dystrophy, among others. BMI technology offers these patients greater independence and a higher quality of life by enabling the control of external devices to communicate with others and the ability to manipulate their environment at will (Wolpaw, Birbaumer, McFarland, Pfurtscheller, & Vaughan, 2002).

There are two types of BMI: invasive BMI and noninvasive BMI. Invasive BMI requires surgical procedures and measures the brain signals from intracranial electrodes (needle electrodes or brain surface electrodes), whereas noninvasive BMI measures brain signals noninvasively from outside of the body using scalp electrodes, and so forth. To achieve a higher performance and a higher level of usefulness, we employed invasive BMI techniques, which involve the implantation of devices. For use in a practical situation, invasive BMI requires an organic integration of the following medical and engineering technologies:

1) Neural recording with high spatiotemporal resolution
2) High-speed data transfer and processing
3) Optimal extraction of appropriate neurophysiological features
4) Accurate neural decoding

5) Robust control of external devices such as robotic arms and electric wheelchairs
6) Downsizing, integration, and implantation of electronic devices, and the use of wireless technology
7) Noninvasive pre-surgical evaluations for appropriate surgical indications
8) On-target survey and analysis of patient needs
9) Addressing of neuroethical issues

In this chapter, we describe the development of our invasive BMI system using brain surface electrodes.

Figure 1. A conceptual diagram of the brain machine interface.

NEURAL DECODING AND REAL-TIME ROBOTIC CONTROL USING ELECTROCORTICOGRAMS

Clinical studies using electrocorticograms recorded from brain surface electrodes

In the process of providing neurosurgical treatments for specific groups of patients, we sometimes record brain signals (**electrocorticograms**: ECoGs) or electrically stimulate the brain using electrodes that are directly placed on the brain surface. The ECoGs can selectively measure brain signals within a limited distance of a few millimeters without distortion. In addition, the ECoGs are insusceptible to external noises, and the scalp skin electrodes measure the distorted brain signals (electroencephalograms: EEGs) from a distance of up to a few centimeters. Furthermore, ECoG recordings from the brain surface electrodes are stable for at least one year (Chao, Nagasaka, & Fujii, 2010), whereas the spike recordings from the needle electrodes will gradually deteriorate in yield due to chronic inflammatory tissue reactions. The ECoG is a well-balanced brain signal for BMI (Table 1). Thus, we prefer to use the ECoGs recorded by the brain surface electrodes for BMI to achieve a high performance.

In our clinical studies, all of the subjects were recruited from patients in whom we temporarily placed brain surface electrodes to treat intractable pain or epilepsy. Informed consent was obtained from all of the patients, and all of the studies were performed with the approval of the ethics committee of Osaka University Medical Hospital. We measured the ECoGs during the performance of two or three types of simple motor tasks of the hand or arm, such as grasping, pinching, and elbow flexion. We predicted the type of movement based on the analysis of a single ECoG trial using a **support vector machine** (SVM) algorithm (Kamitani & Tong, 2005). As a result, we were able to predict movement types on a single trial basis with an accuracy rate of 70-90%. Specifically, we first demonstrated that ECoGs from the anterior wall of the central sulcus (a groove in the brain where most of the primary motor cortex lies) are useful for the accurate and early decoding of movement types (Yanagisawa et al., 2009). Most of the primary motor cortex, which is responsible for the final functional output of motor commands, lies within the anterior wall of the central sulcus. In humans, the anterior wall of the central sulcus contains many neurons that directly project to the spinal anterior horn cells, and such neurons are thought to be related to fine movement control (Rathelot & Strick, 2009). We suggest that an appropriate neurophysiological feature extraction from the central sulcus contributed to our accurate movement decoding.

We applied this decoding method to an ECoG-based BMI system for real-time control of a robotic arm (Figure 2). The ECoGs were measured using a 128-channel digital EEG system (EEG 2000; Nihon Koden Corporation, Tokyo, Japan) and digitized at a sampling rate of 1000 Hz. We introduced successive decoding every 200 ms, and the **Gaussian process regression** was used to predict the movement onset. Next, the SVM was used to infer the type of hand and arm movements. The robotic arm was an experimental anthropomorphic hand developed by Prof. Yokoi H(Yokoi, Kita, & Nakamura, 2009). The general movement mechanisms and degrees of freedom of the hand mimicked those of a human hand. In addition, the hand was equipped with 8 DC motors to independently actuate 8 individual tendons in the robotic hand. The 8 tendons functioned in a coordinated manner to accomplish flexion or extension of each individual finger. As a result, we found that the normalized power in the high **gamma band** (80 -

150 Hz) gave the highest decoding accuracy of all the frequency bands and ranged from 3 to 150 Hz (Yanagisawa et al., 2011). We succeeded in generating the voluntary control of grasping and releasing of objects (Figure 3) (Yanagisawa et al., in press). Using a successive decoding and control algorithm, a smooth robotic hand movement was achieved, although the decoding accuracy on a single trial basis was approximately 70%. We found that despite being severely paralyzed, just the imagery of the hand movement could induce clear, high gamma band responses that were similar to those induced by real movements.

Table 1. Brain signals used for the Brain-Machine Interface.

Figure 2. A real-time BMI system for robotic arm control.

Figure 3. Real-time control of a robotic arm. The patient voluntarily controlled grasping (right) and opening (left) of the robotic arm in real time.

A FULLY IMPLANTABLE WIRELESS SYSTEM

Wired leads, which penetrate the skin, pose a high risk of infection. It is necessary to fully implant a recording system within the body to reduce the infection risk from the penetration of wire leads. Moreover, once the devices are implanted, it will be more convenient to use the BMI system because the patients would not have to wear or remove the system. For this reason, we have developed the first prototype of a fully implantable ECoG recording system for human brain-machine interfaces using brain surface electrodes. By integrating this wireless system into a real-time BMI system, we ultimately aim to develop a Wireless Human ECoG-based Real-time BMI System (W-HERBS) (Hirata et al., 2011).

System Overview

The first prototype is shown in Figure 4. This fully implantable system includes many new technologies such as a 64-ch integrated analog amplifier chip, a Bluetooth wireless data transfer circuit, a wirelessly rechargeable battery, 3-dimensional tissue conformable high-density electrodes, a titanium head casing, and a fluorine polymer body casing.

The implantable system consists of two parts; a head part and a body part. The head part consists of tissue conformable brain surface microelectrodes, a titanium head casing that also functions as an artificial skull, and a 128-ch amplifier unit with 2 64-ch chips. The body part consists of a wireless data transfer unit and a microchip data controller, a wireless rechargeable unit, and a fluorine polymer body casing.

Figure 4. A: The first prototype of a fully implantable wireless system for the W-HERBS. A fluorine polymer body casing, which includes a wireless rechargeable unit and a wireless data transfer unit (a). A titanium head casing / artificial skull (b). Brain surface microelectrodes conformable to the outer surface of the individual brain (c). Brain surface microelectrodes conformable to the brain groove (d). B: The prototype is attached to the skull bone model.

Integrated Analog Amplifier Unit

The ECoG is characterized as signals with low frequency bands that range from 0.1 Hz to 500 Hz and produces small amplitudes that range from 1 μV to 1 mV. It is necessary to reduce the input-referred noise of the amplifier to record the ECoG signals (Yoshida et al., 2010). The variable bandwidth and wide dynamic ranges are also important because commercial AC noises with similar frequency bands can easily contaminate ECoG signals. Thus, a high-linearity low noise amplifier with a variable bandwidth was developed to cover the frequency bands and voltage gains appropriate for recording ECoG signals

(Yoshida et al., 2011). The low noise amplifier with a 0.1 Hz roll-off frequency was implemented with core differential amplifiers using large-sized MOSFETs and a capacitor feedback scheme biased by ultrahigh resistors of cascade 12 MOSFETs. A VLSI chip was fabricated using CMOS 0.18 μm process technology in the chip fabrication program of the VLSI Design and Education Center (VDEC) at the University of Tokyo.

The specifications of the chip functions are as follows:

- number of channels: 64 channels
- 12 bits A/D converter
- voltage gain: 40 – 80 dB
- signal frequency bands: 0.1 – 1000 Hz
- input referred noise: 2.8 μV
- power consumption: 4.9 mW
- chip size: 5.0 mm x 5.0 mm
- master/slave function for a 128-channel system

A 128-channel analog amplifier board consists of two chips mounted on two high-density printed boards that were bridged by flexible printed wiring (Figure 5). The size of the board was 20 mm x 30 mm x 2.5 mm, which was small enough to be placed within a head casing, which will be described later in the text.

Figure 5. A 128-channel integrated analog amplifier board

Wireless Data Transfer Unit

We adapted the **Bluetooth** protocol communication (Class 2) for the first prototype for its high usability. A combination of 2 sets of Bluetooth circuits enabled us to achieve effective data transmission rates of 400 kbps, which allowed the transfer of 128-ch x 12-bit ECoG data in real time. Power consumption was approximately 300 mW, which meant that most of the system power was consumed by the wireless data transfer. Further improvements in the data transfer protocol should be made to achieve a faster and more power-efficient operation of the system. The size was 60 mm x 60 mm x 8 mm, which should also be reduced. One solution would be to change the data transfer protocol from Bluetooth to WLAN or UWB.

Wireless Rechargeable Unit

The wireless battery charging system consists of two parts. One is a transmitter positioned outside of the human body, and the other is a receiver located inside the human body. We achieved a wireless charging power of 4 W at a distance of 38 mm, which was sufficient to run the entire implantable system. The coil size of the abdominal portion was 40 mm in diameter and 8 mm in thickness, which may be scaled down if the power consumption can be reduced.

Tissue Conformable Brain Surface Microelectrodes

To record the ECoGs with a higher spatiotemporal resolution, we developed 3-dimensional high-density grid electrodes, which were designed to fit to the individual's brain surface (Hirata et al., 2010). We extracted 3-dimensional (3D) surface data of the brain surface and brain groove from the patient's individual magnetic resonance (MR) images. An automatic brain groove extraction software program (Brain VISA, http://brainvisa.info/) was used. Next, we designed male and female molds for the grid electrodes using 3D CAD software (3 matic, Materialize Japan, Tokyo, Japan) (Figure 6). Next, the molds were rapidly produced by a 3D printer. The silicon sheets fitting the brain surface were subsequently produced from these molds. In addition, the location of each platinum electrode (1.0 mm in diameter) was designed with the 3D CAD software, which took into account the individual's anatomical information. The inter-electrode spacing was up to 2.5 mm and the brain groove grid electrodes were located on both sides of the electrode sheet. These 3D grid electrodes fitted onto the brain surface with only a minimal

compression of the brain tissue and generated high ECoGs yields due to their close contact with the brain surface.

Figure 6. Tissue conformable brain surface microelectrodes. The tissue conformable brain surface microelectrodes fitted on to the individual brain surfaces. Left: High-density electrodes (inter-electrode spacing 2.5 mm) and standard electrodes (inter-electrode spacing 10 mm). Middle: Gyral (brain surface) electrodes. Right: Sulcal (brain groove) electrodes.

Head Casing and Artificial Skull Bone

We developed a titanium head casing, which contained a 128-channel amplifier unit. This casing functioned as both a head casing and an artificial skull bone and was designed to fit a patient's individual skull bone shape using the 3D CAD (3 matic, Materialize Japan, Tokyo) and 3D CAM (Gibbs CAM, Gibbs and Associates, USA) software programs (Figure 7). This head casing not only had cosmetic advantages, but it was also safer than other convex shapes that posed a higher risk of cutaneous fistula.

Figure 7. A titanium head casing / artificial skull bone. A: A computer simulation of machining path using 3D CAM software. B: A computer simulation of a head casing fitting the skull bone. Left: skull bone opening. Middle: Outer side view of a head casing fitting the skull bone. Right: Inner side view. C: A head casing designed using 3D CAD software. Upper: A head casing without an electronic circuit board. Lower: A head casing with an electronic circuit board. D: A prototype casing. Upper: inner side view. Lower: outer side view. E: A prototype casing attached to the skull bone model. Three-dimensional skull bone data were obtained from the individual's CT images. The head casing contains two 64-channel integrated amplifier chips on a small mounting board, which was mounted onto a folded inner panel as indicated by the green color.

Fluorine Polymer Body Casing

Compared with the head casing, the body casing offers a larger space and does not require careful cosmetic consideration. We introduced a soft casing made of **fluorine polymer**, which has advantages in terms of cost, chemical stability, durability, and biocompatibility. This body casing embeds a wireless data transfer unit and a microchip data controller, a wireless power supply unit, and a rechargeable battery in silicone covered by fluorine polymer films.

NONINVASIVE NEURAL DECODING USING MAGNETOENCEPHALOGRAPHY

A noninvasive evaluation of the individual BMI performance is indispensable for determining the surgical indication of the invasive BMI treatment. A **magnetoencephalography** (MEG) is a potentially noninvasive method for evaluating individual BMI performance because of its high spatiotemporal resolution and neurophysiological compatibility with the ECoG. We investigated the neural decoding performance of 3 types of unilateral hand and arm movements on a single trial basis using an MEG (Sugata et al., 2012). We used an SVM to decode the movement types. The peak amplitudes of the first component after the movement onset of the movement-related cortical fields (pMRCF) were used as decoding features. As a result, the neural decoding accuracies largely exceeded the chance level in all of the 9 healthy subjects that were evaluated. The pMRCFs and decoding accuracies were strongly correlated ($rs = 0.900$, $p = 0.002$) (Figure 8). These results suggested that the neurophysiological profiles might serve as a predictor of individual BMI performance and assist in the improvement of general BMI performance.

Figure 8. Neural decoding using magnetoencephalography. A: a typical averaged waveform of a movement-related cortical field. B: The relationship between the neural decoding accuracies and the peak amplitudes of the first component after the movement onset of the movement-related cortical field.

CONCLUSION

We have developed an ECoG-based real-time BMI system and the first prototype of a fully implantable wireless system. The ECoG-based real-time BMI system successfully provided voluntary control over the grasping and opening of a robotic hand. A fully implantable wireless system is indispensable for the clinical application of invasive BMI to reduce the risk of infection. The noninvasive evaluation of an individual BMI performance using an MEG might be useful for determining the surgical indication of invasive BMI treatment.

ACKNOWLEDGMENTS

This work was supported by the Strategic Research Program for Brain Sciences of MEXT. We would like to acknowledge Atsushi Iwata (A-R-Tec Corp.), Shinichi Morikawa, Yoshihiro Watanabe (Unique Medical), Naohiro Hayaishi (Keisuugiken Corp.), Shinichi Yoshimura, Shuhei Kosaka (Aska Electric Co. Ltd.), and Hirofumi Itoh (Junkosha Inc.) for prototype manufacturing of our implantable system, and we would also like to thank the VLSI Design and Education Center (VDEC) and the University of Tokyo for their help with the chip fabrication program.

REFERENCES

Chao, Z. C., Nagasaka, Y., & Fujii, N. (2010). Long-term asynchronous decoding of arm motion using electrocorticographic signals in monkeys. *Front Neuroengineering, 3*, 3.

Hirata, M., Matsushita, K., Suzuki, T., Yoshida, T., Sato, F., Morris, S., et al. (2011). A fully-implantable wireless system for human brain-machine interfaces using brain surface electrodes: W-HERBS. *IEICE Trans Commun, E94-B*, 2448-2453.

Hirata, M., Yoshimine, T., Saitoh, Y., Yanagisawa, T., Goto, T., Watanabe, Y., et al. (2010). US patent Patent No. US7,860,577.

Kamitani, Y., & Tong, F. (2005). Decoding the visual and subjective contents of the human brain. *Nat Neurosci, 8*(5), 679-685.

Rathelot, J. A., & Strick, P. L. (2009). Subdivisions of primary motor cortex based on cortico-motoneuronal cells. *Proc Natl Acad Sci U S A, 106*(3), 918-923.

Sugata, H., Goto, T., Hirata, M., Yanagisawa, T., Shayne, M., Matsushita, K., et al. (2012). Movement-related neuromagnetic fields and performances of single trial classifications. *Neuroreport, 23*(1), 16-20.

Wolpaw, J. R., Birbaumer, N., McFarland, D. J., Pfurtscheller, G., & Vaughan, T. M. (2002). Brain-computer interfaces for communication and control. *Clin Neurophysiol, 113*(6), 767-791.

Yanagisawa, T., Hirata, M., Saitoh, Y., Goto, T., Kishima, H., Fukuma, R., et al. (2011). Real-time control of a prosthetic hand using human electrocorticography signals. *J Neurosurg, 114*(6), 1715-1722.

Yanagisawa, T., Hirata, M., Saitoh, Y., Kato, A., Shibuya, D., Kamitani, Y., et al. (2009). Neural decoding using gyral and intrasulcal electrocorticograms. *Neuroimage, 45*(4), 1099-1106.

Yanagisawa, T., Hirata, M., Saitoh, Y., Kishima, H., Matsushita, K., Goto, T., et al. (in press). Electrocorticographic control of a prosthetic arm in paralyzed patients. *Ann Neurol.*

Yokoi, H., Kita, K., & Nakamura, T. (2009). Mutually Adaptable EMG Devices for Prosthetic Hand. *The International Journal of Factory Automation, Robotics and Soft Computing*, 74-83.

Yoshida, T., Masui, Y., Eki, R., Iwata, A., M., Y., & Uematsu, K. (2010). A Neural Recording Amplifier with Low-Frequency Noise Suppression. *IEICE Trans. Electrons, E93-C*, 849-854.
Yoshida, T., Sueishi, K., Iwata, A., Matsushita, K., Hirata, M., & Suzuki, T. (2011). A High-Linearity Low-Noise Amplifier with Variable Bandwidth for Neural Recording Systems. *Japanese Journal of Applied Physics, 50*(4).

ADDITIONAL READING SECTION

Birbaumer, N., & Cohen, L. G. (2007). Brain-computer interfaces: communication and restoration of movement in paralysis. *J Physiol, 579*(Pt 3), 621-636.
Birbaumer, N., Weber, C., Neuper, C., Buch, E., Haapen, K., & Cohen, L. (2006). Physiological regulation of thinking: brain-computer interface (BCI) research. *Prog Brain Res, 159*, 369-391.
Brunner, P., Bianchi, L., Guger, C., Cincotti, F., & Schalk, G. (2011). Current trends in hardware and software for brain-computer interfaces (BCIs). *J Neural Eng, 8*(2), 025001.
Brunner, P., Ritaccio, A. L., Emrich, J. F., Bischof, H., & Schalk, G. (2011). Rapid Communication with a "P300" Matrix Speller Using Electrocorticographic Signals (ECoG). *Front Neurosci, 5*, 5.
Buch, E., Weber, C., Cohen, L. G., Braun, C., Dimyan, M. A., Ard, T., et al. (2008). Think to move: a neuromagnetic brain-computer interface (BCI) system for chronic stroke. *Stroke, 39*(3), 910-917.
Felton, E. A., Wilson, J. A., Williams, J. C., & Garell, P. C. (2007). Electrocorticographically controlled brain-computer interfaces using motor and sensory imagery in patients with temporary subdural electrode implants. Report of four cases. *J Neurosurg, 106*(3), 495-500.
Guenther, F. H., Brumberg, J. S., Wright, E. J., Nieto-Castanon, A., Tourville, J. A., Panko, M., et al. (2009). A wireless brain-machine interface for real-time speech synthesis. *PLoS One, 4*(12), e8218.
Hashimoto, Y., Ushiba, J., Kimura, A., Liu, M., & Tomita, Y. (2010). Change in brain activity through virtual reality-based brain-machine communication in a chronic tetraplegic subject with muscular dystrophy. *BMC Neurosci, 11*, 117.
Hochberg, L. R., Serruya, M. D., Friehs, G. M., Mukand, J. A., Saleh, M., Caplan, A. H., et al. (2006). Neuronal ensemble control of prosthetic devices by a human with tetraplegia. *Nature, 442*(7099), 164-171.
Jackson, A., Mavoori, J., & Fetz, E. E. (2006). Long-term motor cortex plasticity induced by an electronic neural implant. *Nature, 444*(7115), 56-60.
Jarosiewicz, B., Chase, S. M., Fraser, G. W., Velliste, M., Kass, R. E., & Schwartz, A. B. (2008). Functional network reorganization during learning in a brain-computer interface paradigm. *Proc Natl Acad Sci U S A, 105*(49), 19486-19491.
Jochum, T., Denison, T., & Wolf, P. (2009). Integrated circuit amplifiers for multi-electrode intracortical recording. *J Neural Eng, 6*(1), 012001.
Kellis, S. S., House, P. A., Thomson, K. E., Brown, R., & Greger, B. (2009). Human neocortical electrical activity recorded on nonpenetrating microwire arrays: applicability for neuroprostheses. *Neurosurg Focus, 27*(1), E9.
Krusienski, D. J., Grosse-Wentrup, M., Galan, F., Coyle, D., Miller, K. J., Forney, E., et al. (2011). Critical issues in state-of-the-art brain-computer interface signal processing. *J Neural Eng, 8*(2), 025002.
Kubanek, J., Miller, K. J., Ojemann, J. G., Wolpaw, J. R., & Schalk, G. (2009). Decoding flexion of individual fingers using electrocorticographic signals in humans. *J Neural Eng, 6*(6), 66001.
Lebedev, M. A., & Nicolelis, M. A. (2006). Brain-machine interfaces: past, present and future. *Trends Neurosci, 29*(9), 536-546.
Leuthardt, E. C., Gaona, C., Sharma, M., Szrama, N., Roland, J., Freudenberg, Z., et al. (2011). Using the electrocorticographic speech network to control a brain-computer interface in humans. *J Neural Eng, 8*(3), 036004.
McFarland, D. J., Krusienski, D. J., & Wolpaw, J. R. (2006). Brain-computer interface signal processing at the Wadsworth Center: mu and sensorimotor beta rhythms. *Prog Brain Res, 159*, 411-419.

Mellinger, J., Schalk, G., Braun, C., Preissl, H., Rosenstiel, W., Birbaumer, N., et al. (2007). An MEG-based brain-computer interface (BCI). *Neuroimage, 36*(3), 581-593.

Miller, K. J. (2010). Broadband spectral change: evidence for a macroscale correlate of population firing rate? *J Neurosci, 30*(19), 6477-6479.

Miller, K. J., Abel, T. J., Hebb, A. O., & Ojemann, J. G. (2011). Reorganization of large-scale physiology in hand motor cortex following hemispheric stroke. *Neurology, 76*(10), 927-929.

Miller, K. J., Leuthardt, E. C., Schalk, G., Rao, R. P., Anderson, N. R., Moran, D. W., et al. (2007). Spectral changes in cortical surface potentials during motor movement. *J Neurosci, 27*(9), 2424-2432.

Miller, K. J., Schalk, G., Fetz, E. E., den Nijs, M., Ojemann, J. G., & Rao, R. P. (2010). Cortical activity during motor execution, motor imagery, and imagery-based online feedback. *Proc Natl Acad Sci U S A, 107*(9), 4430-4435.

Miller, K. J., Zanos, S., Fetz, E. E., den Nijs, M., & Ojemann, J. G. (2009). Decoupling the cortical power spectrum reveals real-time representation of individual finger movements in humans. *J Neurosci, 29*(10), 3132-3137.

Miyawaki, Y., Uchida, H., Yamashita, O., Sato, M. A., Morito, Y., Tanabe, H. C., et al. (2008). Visual image reconstruction from human brain activity using a combination of multiscale local image decoders. *Neuron, 60*(5), 915-929.

Murguialday, A. R., Hill, J., Bensch, M., Martens, S., Halder, S., Nijboer, F., et al. (2011). Transition from the locked in to the completely locked-in state: a physiological analysis. *Clin Neurophysiol, 122*(5), 925-933.

Musallam, S., Bak, M. J., Troyk, P. R., & Andersen, R. A. (2007). A floating metal microelectrode array for chronic implantation. *J Neurosci Methods, 160*(1), 122-127.

Pei, X., Leuthardt, E. C., Gaona, C. M., Brunner, P., Wolpaw, J. R., & Schalk, G. (2011). Spatiotemporal dynamics of electrocorticographic high gamma activity during overt and covert word repetition. *Neuroimage, 54*(4), 2960-2972.

Pistohl, T., Ball, T., Schulze-Bonhage, A., Aertsen, A., & Mehring, C. (2008). Prediction of arm movement trajectories from ECoG-recordings in humans. *J Neurosci Methods, 167*(1), 105-114.

Rickert, J., Oliveira, S. C., Vaadia, E., Aertsen, A., Rotter, S., & Mehring, C. (2005). Encoding of movement direction in different frequency ranges of motor cortical local field potentials. *J Neurosci, 25*(39), 8815-8824.

Sato, M. A., Yoshioka, T., Kajihara, S., Toyama, K., Goda, N., Doya, K., et al. (2004). Hierarchical Bayesian estimation for MEG inverse problem. *Neuroimage, 23*(3), 806-826.

Schalk, G. (2010). Can Electrocorticography (ECoG) Support Robust and Powerful Brain-Computer Interfaces? *Front Neuroengineering, 3*, 9.

Schalk, G., Kubanek, J., Miller, K. J., Anderson, N. R., Leuthardt, E. C., Ojemann, J. G., et al. (2007). Decoding two-dimensional movement trajectories using electrocorticographic signals in humans. *J Neural Eng, 4*(3), 264-275.

Schalk, G., Miller, K. J., Anderson, N. R., Wilson, J. A., Smyth, M. D., Ojemann, J. G., et al. (2008). Two-dimensional movement control using electrocorticographic signals in humans. *J Neural Eng, 5*(1), 75-84.

Schwartz, A. B. (2004). Cortical neural prosthetics. *Annu Rev Neurosci, 27*, 487-507.

Schwartz, A. B., Cui, X. T., Weber, D. J., & Moran, D. W. (2006). Brain-controlled interfaces: movement restoration with neural prosthetics. *Neuron, 52*(1), 205-220.

Schwartz, A. B., Moran, D. W., & Reina, G. A. (2004). Differential representation of perception and action in the frontal cortex. *Science, 303*(5656), 380-383.

Shenoy, P., Miller, K. J., Ojemann, J. G., & Rao, R. P. (2008). Generalized features for electrocorticographic BCIs. *IEEE Trans Biomed Eng, 55*(1), 273-280.

Toda, A., Imamizu, H., Kawato, M., & Sato, M. A. (2011). Reconstruction of two-dimensional movement trajectories from selected magnetoencephalography cortical currents by combined sparse Bayesian methods. *Neuroimage, 54*(2), 892-905.

Ushiba, J. (2010). Brain-machine interface--current status and future prospects. *Brain Nerve, 62*(2), 101-111.

Vansteensel, M. J., Hermes, D., Aarnoutse, E. J., Bleichner, M. G., Schalk, G., van Rijen, P. C., et al. (2010). Brain-computer interfacing based on cognitive control. *Ann Neurol, 67*(6), 809-816.
Velliste, M., Perel, S., Spalding, M. C., Whitford, A. S., & Schwartz, A. B. (2008). Cortical control of a prosthetic arm for self-feeding. *Nature, 453*(7198), 1098-1101.
Waldert, S., Pistohl, T., Braun, C., Ball, T., Aertsen, A., & Mehring, C. (2009). A review on directional information in neural signals for brain-machine interfaces. *J Physiol Paris, 103*(3-5), 244-254.
Waldert, S., Preissl, H., Demandt, E., Braun, C., Birbaumer, N., Aertsen, A., et al. (2008). Hand movement direction decoded from MEG and EEG. *J Neurosci, 28*(4), 1000-1008.
Whittingstall, K., & Logothetis, N. K. (2009). Frequency-band coupling in surface EEG reflects spiking activity in monkey visual cortex. *Neuron, 64*(2), 281-289.
Wolpaw, J. R. (2007). Brain-computer interfaces as new brain output pathways. *J Physiol, 579*(Pt 3), 613-619.
Wolpaw, J. R., & McFarland, D. J. (2004). Control of a two-dimensional movement signal by a noninvasive brain-computer interface in humans. *Proc Natl Acad Sci U S A, 101*(51), 17849-17854.
Wu, M., Wisneski, K., Schalk, G., Sharma, M., Roland, J., Breshears, J., et al. (2010). Electrocorticographic frequency alteration mapping for extraoperative localization of speech cortex. *Neurosurgery, 66*(2), E407-409.
Yamashita, O., Sato, M. A., Yoshioka, T., Tong, F., & Kamitani, Y. (2008). Sparse estimation automatically selects voxels relevant for the decoding of fMRI activity patterns. *Neuroimage, 42*(4), 1414-1429.

KEY TERMS AND DEFINITIONS

Brain-machine interface: a man-machine interface, which enables us to control machines and to communicate with others without the use of input devices, but through the direct use of brain signals alone.
Neural decoding: decoding neural signals.
Real time: to respond on the order of milliseconds and at times, microseconds.
Prosthetic arm: an artificial robotic arm that substitutes for a missing arm.
Implantable device: a medical device implanted within the body.
Brain surface electrodes: electrodes that are directly placed on the brain surface.
Motor restoration: recovery of neural motor function.

Movement-related neuromagnetic fields and performances of single trial classifications

Hisato Sugata[a], Tetsu Goto[a,b], Masayuki Hirata[a,b], Takufumi Yanagisawa[b,c], Morris Shayne[b], Kojiro Matsushita[b], Toshiki Yoshimine[b] and Shiro Yorifuji[a]

In order to clarify whether neurophysiological profiles affect the performance of brain machine interfaces (BMI), we examined the relationships between amplitudes of movement-related cortical fields (MRCFs) and decoding performances during movement. Neuromagnetic activities were recorded in nine healthy participants during three types of unilateral upper limb movements. The movement types were inferred by a support vector machine. The amplitude of MRCF components, motor field (MF), movement-evoked field I (MEFI), and movement-evoked field II (MEFII) were compared with the decoding accuracies in all participants. Decoding accuracies at the latencies of MF, MEFI, and MEFII surpassed the chance level in all participants. In particular, accuracies at MEFI and MEFII were significantly higher in comparison with that of MF. The amplitudes and decoding accuracies were strongly correlated (MF, $r_s=0.90$; MEFI, $r_s=0.90$; and MEFII, $r_s=0.87$). Our results show that the variation of MRCF components among participants reflects decoding performance. Neurophysiological profiles may serve as a predictor of individual BMI performance and assist in the improvement of general BMI performance. *NeuroReport* **23:16–20 © 2011 Wolters Kluwer Health | Lippincott Williams & Wilkins.**

NeuroReport 2012, **23**:16–20

Keywords: brain machine interface, magnetoencephalography, movement-related cortical fields, neural decoding

[a]Division of Functional Diagnostic Science, Osaka University Graduate School of Medicine, [b]Department of Neurosurgery, Osaka University Medical School, Osaka and [c]ATR Computational Neuroscience Laboratories, Kyoto, Japan

Correspondence to Masayuki Hirata, MD, PhD, Department of Neurosurgery, Osaka University Medical School, 2-2 E6 Yamadaoka, Suita, Osaka 565-0871, Japan
Tel: +81 668 793 652; fax: +81 668 793 659;
e-mail: mhirata@nsurg.med.osaka-u.ac.jp

Received 10 September 2011 **accepted** 27 September 2011

Introduction

Brain machine interfaces (BMI) utilize brain signals for controlling external devices such as computers and prostheses [1–4]. This technology is expected to restore motor function to severely paralyzed patients with amyotrophic lateral sclerosis or high cervical cord injury. To realize clinical applications of BMI, many studies have examined the validity of measuring brain activities [2–6], and recent advancements in methods for evaluating neural activity and neural decoding have led to increased decoding performances, even when using noninvasive methods such as electroencephalography and magnetoencephalography (MEG) [7–9]. However, there have been few studies discussing the neurophysiological significance of brain signals contributing to classifications.

Neurophysiological activities related to movement can be measured with high spatiotemporal resolution using MEG. These are known as movement-related cortical fields (MRCFs) [10,11]. Many MEG studies reported signal component generators for the various MRCFs [12–14]. MRCFs consist of three components: the readiness field, motor field (MF), and movement-evoked fields (MEF). The readiness field is thought to reflect activities in the supplementary motor area during preparation periods for movements, and both the MF and MEFs reflect activities in the sensorimotor areas during movement [15]. Furthermore, the MEF consists of three components, numbered from I to III. MEFI is the first negative response, and has been proposed to represent sensory feedback from muscle spindles to the primary somatosensory cortex [16]. MEFII and MEFIII are positive and negative responses, respectively, and are observed within 500 ms after movement onset [11]. MEFII is thought to represent the second activation of the precentral gyrus in close proximity to the anterior wall within the central sulcus [13], whereas the generator of MEFIII remains unclear.

MEG studies have demonstrated that different participants exhibit different MRCFs patterns. For example, the MF is not always observed and its pattern depends on movement type [16]. In addition, not all three MEF components may be identified in all participants [17].

The aim of this study was to examine the relationship between the decoding performance and the neurophysiological profiles of MRCFs. For this purpose, we focused on MF, MEFI, and MEFII and evaluated these components to examine the relationship between the amplitude of each of the MRCF components and the decoding accuracy calculated using them.

Supplemental digital content is available for this article. Direct URL citations appear in the printed text and are provided in the HTML and PDF versions of this article on the journal's Website (*www.neuroreport.com*).

0959-4965 © 2011 Wolters Kluwer Health | Lippincott Williams & Wilkins

DOI: 10.1097/WNR.0b013e32834d935a

Materials and methods

Participants

Nine right handed healthy volunteers participated in the study (four men and five women; mean age 32.8 years, SD 14.2, range 21–59 years). All participants had no history of neurological or psychiatric diseases. In accordance with the Declaration of Helsinki, we explained the purpose and possible consequences of this study to all participants and obtained written informed consent before their study participation. The protocol of this study was approved by the ethics committee of the Osaka University Hospital.

Task

The experimental paradigm is shown in Fig. 1. An epoch started with a 4-s resting state and visual presentation of a black fixation cross. Then, a Japanese word representing one of the three movements (grasping, pinching, and elbow flexion) was presented to instruct the participant which movement to perform after the execution-cue. Each of the three movements was performed 60 times, and the movement in any given epoch was selected randomly.

Measurements and preprocessing

Neuromagnetic activities were recorded in a magnetically shielded room using a 160-channel whole-head MEG system equipped with coaxial type gradiometers (MEG vision NEO; Yokogawa Electric Corporation, Kanazawa, Japan). The participant lay on a bed in the supine position with their head centered. Visual stimuli were displayed on a projection screen using a visual presentation system (Presentation; Neurobehavioral Systems, Albany, California, USA) and a liquid crystal projector (LVP-HC6800; Mitsubishi Electric, Tokyo, Japan). Data were sampled at a rate of 1000 Hz with an online low-pass-filter at 200 Hz. After data acquisition, a notch filter at 60 Hz was applied to eliminate the AC line noise. To reduce contamination from muscle activities and eye movements, we instructed the participants to rest their elbows on a cushion while avoiding shoulder movements, and to watch the center of the display without ocular movements or blinking. We also recorded electromyograms of the flexor pollicis brevis, flexor digitorum superficialis, and biceps brachii muscles. Each movement onset was determined by an initial rise in the most responsive electromyogram waveforms, and this onset time was defined as 0 ms. Normalized neuromagnetic amplitudes of epochs from −4000 to 2000 ms were calculated by subtracting the mean and dividing by SD of the baseline values (−4000 to −3000 ms). As channels for analysis, all MEG channels were selected except those of the bilateral frontal base, which were omitted in order to minimize such artifact contamination as eye movements and/or eye blinking.

Fig. 1

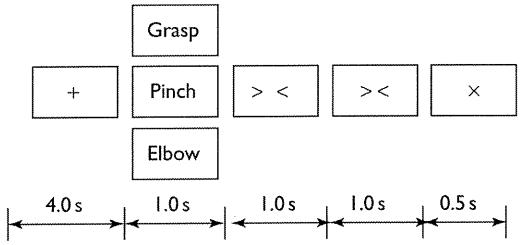

Experimental paradigm. An epoch began with a 4-s resting phase and visual presentation of a black fixation cross. A Japanese word representing one of three movements was then presented for 1 s to instruct the participant which movement to perform after the execution-cue. Two 1-s timing-cues were presented before the execution-cue. Each of the three movements was performed 60 times.

Evaluation of amplitude of movement-related cortical fields

In order to reveal the relationship between responses of MRCF components and decoding performances, we evaluated the amplitude of three MRCF components and compared these values with the decoding accuracy. After checking the emergence of MRCF components on channels over the sensorimotor area in all participants (Fig. 2a), we obtained the grand field powers of MF, MEFI, and MEFII for each of the three movements in each participant. To calculate these powers, we used the root mean square (RMS), which was calculated from the averaged wave forms of all MEG channels used for analysis. Three detectable peaks of RMS amplitudes corresponding to the latencies of MF, MEFI, and MEFII were defined as the grand field powers of each MRCF component (Fig. 2b). Next, the mean of these powers for the three movements were measured for each component, and this mean power for each component was used as the participant's amplitude of response. The supplementary Table, Supplemental digital content 1, *http://links.lww.com/WNR/A168* shows the mean latencies and the amplitudes for the three components in all participants. Then, single trial classification of movements was performed using the averaged normalized neuromagnetic amplitudes as a decoding feature. These amplitudes were calculated for each channel between −25 and +25 ms from the latencies for each of the three components. Furthermore, a univariate statistical analysis of each decoding feature was performed to reveal which channel showed statistically significant variability among movement classes. The F value of a one-way analysis of variance was examined across the three classes of movement using the averaged normalized neuromagnetic amplitudes as a decoding feature of MF, MEFI, and MEFII. The topographies of the F values with statistically significant differences ($P < 0.05$) were delineated on a map of all MEG channels.

Classification of movements

A linear support vector machine (SVM), that was extended to discriminate multiclasses [18], was used to classify the movements on Matlab 2008a software

Fig. 2

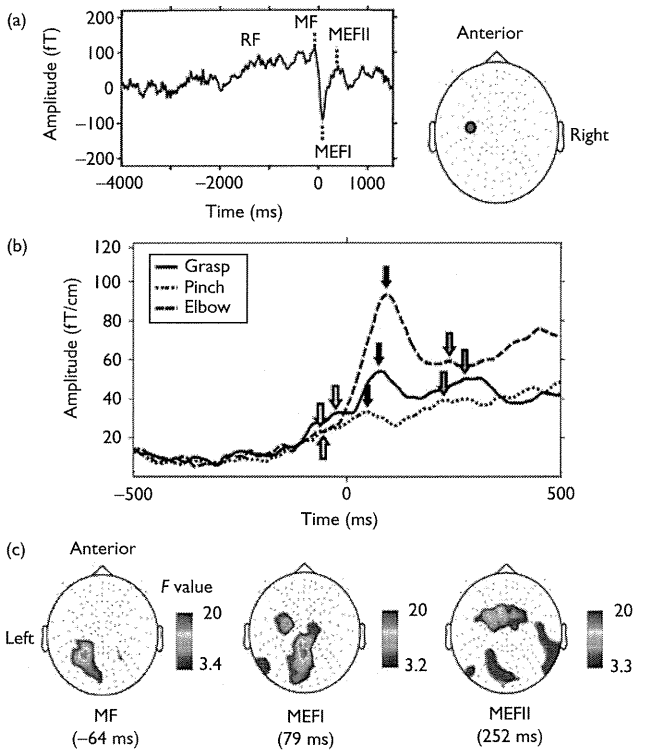

(a) Time average of the movement-related magnetic fields for right grasping movement in one participant for a channel overlying the contralateral sensorimotor area (red circle). MEFI and MEFII, first and second movement-evoked fields; MF, motor field; RF, readiness field. (b) The root mean square amplitudes of motor evoked responses in each of three movements in a same participant. The root mean square curve shows three peaks. These peaks correspond to MF (white arrows), MEFI (black arrows), and MEFII (gray arrows). In each component, the amplitudes and latencies from three movements were averaged. (c) Topographies of *F* values showing differences of the decoding features in each channel in the same participant. Significant differences were observed in the channels located over the parietal area at the latency of MF (left) and over both the parietal area and sensorimotor area at the latency of MEFI (middle). Channels with high *F* values at the latency of MEFII were distributed mainly over the frontal area (right). Color bar shows a range of significant *F* values ($P<0.05$, analysis of variance).

(Mathworks, Natwick, Massachusetts, USA). We used a 10-fold cross-validation as our performance measure. All epochs were divided into 10 blocks and one of the 10 blocks was selected as a testing dataset. A SVM decoder was trained by the trials of the other nine blocks. Then, the testing dataset was used for prediction of movements. This routine was repeated 10 times, and the average percent correct over all runs was presented as a measure of decoder performance. A Mann–Whitney *U*-test was applied to statistically evaluate the differences of decoding accuracies among the three MRCF components. After that, we compared the amplitudes and the decoding accuracies of all participants for each component, and the correlation coefficients were calculated by a Spearman's rank correlation test.

Results

MRCFs were observed on channels over the motor area (Fig. 2a). Three peaks of RMS amplitudes were obtained around movement onset and approximately corresponded to the latencies of MF, MEFI, and MEFII (Fig. 2b). As for the variability of decoding features of each MEG channel, *F* values with statistical significance ($P < 0.05$, analysis of variance) were mainly located in channels over the parietal area at the latency of MF, and in those over the parietal area and the sensorimotor area at the latencies of MEFI and MEFII (Fig. 2c).

With regard to classification of movements, decoding accuracies at the three MRCF components surpassed the chance level in all participants (Fig. 3a). The decoding accuracies at MEFI and MEFII were significantly higher in comparison with that of MF ($P < 0.05$, Mann–Whitney

Fig. 3

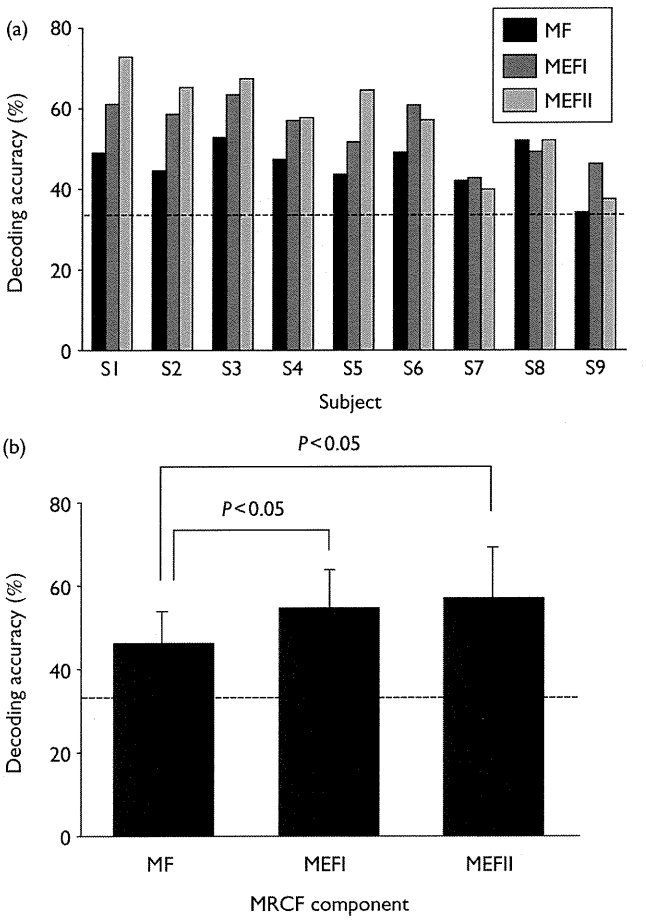

(a) Decoding accuracies at the latencies of MF, MEFI, and MEFII in all participants. Decoding accuracies in most participants exceeded the chance level at each MRCF component. (b) The mean decoding accuracies at the latencies of MEFI and MEFII were significantly higher in comparison with that of MF ($P<0.05$, Mann–Whitney *U*-test). A dotted line indicates the chance level (33.3%). MEFI and MEFII, first and second movement-evoked fields; MF, motor field; MRCF, movement-related cortical field.

Fig. 4

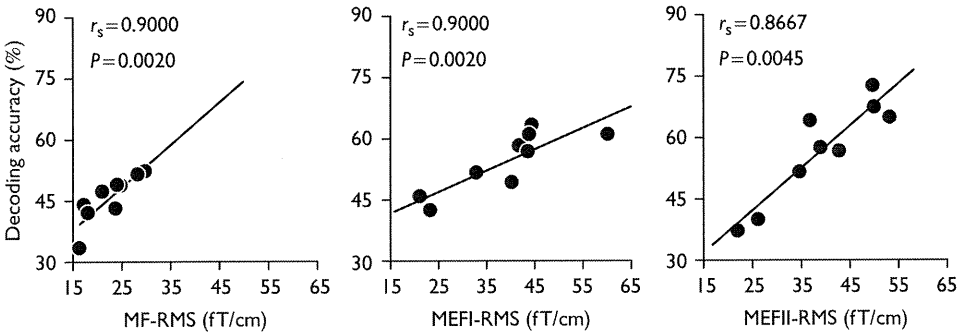

Scatter diagrams showing the correlation between RMS amplitude and decoding accuracy. There were significant positive correlations between amplitudes and the decoding accuracies for all of the three components (MF, r_s=0.90, P<0.005; MEFI, r_s=0.90, P<0.005; MEFII, r_s=0.87, P<0.005; Spearman's rank correlation test). MEFI and MEFII, first and second movement-evoked fields; MF, motor field; RMS, root mean square.

U-test) (Fig. 3b). Furthermore, the relationship between the amplitude for each component of the MRCFs and their decoding accuracies showed a significant positive correlation for all of the three components (Fig. 4; MF, $r_s = 0.90$, $P < 0.005$; MEFI, $r_s = 0.90$, $P < 0.005$; MEFII, $r_s = 0.87$, $P < 0.005$; Spearman's rank correlation test).

Discussion

In this study, we discriminated three types of upper-limb movements based on single-trial MEG signals using an SVM, and compared the decoding accuracy with three MRCF components. Decoding accuracies at these three components largely exceeded the chance level and were strongly correlated with the amplitudes of their responses. These results show a relationship between high decoding accuracy and high amplitudes of the three neurophysiological components. Below, we discuss the MRCFs and the effect on decoding performance.

Individual differences in neuromagnetic fields during movements have been reported in amplitude and spatiotemporal patterns [16,17]. These results suggest the possibility that individual differences in neurophysiological activity may be involved in explaining differences in BMI performance. In our study, the amplitude of all three MRCF components significantly correlated with the decoding accuracy. In addition, decoding accuracies at the latencies of MEFI and MEFII were significantly higher than that of MF. As described above, strong correlations were shown between amplitudes and performances in all components. Especially, in MEFI and MEFII, there were participants with high amplitudes in comparison within MF, and they achieved high decoding performances. Therefore, the amplitude of component derived from individual difference in neurophysiological profiles may affect decoding performances.

Furthermore, significant spatiotemporal differences in the magnetic fields among the three movements were obtained in the frontoparietal MEG channels overlaying the sensorimotor area and parietal area at the latencies of the three components of MRCFs. The sensorimotor and parietal areas have been previously reported to have movement-specific responses [16,19,20]. Our results also showed that MEG channels over these areas contributed to the decoding performance of movement in comparison with other channels. These suggest that brain signals from the sensorimotor and parietal areas have specific information related to movements.

MEG generally shows higher sensitivity to activities in the sulci than to those in the gyri, because currents in the sulci flow tangentially to the skull and thus produce stronger extracranial magnetic fields [21,22]. Therefore, this aspect of MEG is useful for detecting activities in the anterior and posterior walls of the central sulcus, which are the generators of the MF, MEFI, and MEFII [16]. In fact, these three components provided higher decoding accuracy than chance level in our study, indicating the possibility that MEG can detect the information related to the somatotopy of the anterior and posterior walls of the central sulcus. In an electrocorticographic study, signals from the anterior wall of the central sulcus contributed more to discrimination than those from other channels [23]. These findings indicate that the signals within the central sulcus are promising for motor BMI, and that performance of a MEG-based BMI may be a predictor for the performance of an ECoG-based BMI.

To predict the performance of clinical BMI for patients with severe paralyses, it is important to focus on MF. The MF is said to appear also in patients with amyotrophic lateral sclerosis and high cervical spinal cord injury, because the efferent signals from the motor-related area persist in these patients [24,25]. In present study, the accuracy rates at the latency of MF significantly exceeded chance levels. This result indicates that the amplitude of MF also affects BMI performance, suggesting that neurophysiological profiles of MF may be useful in predicting decoding performance before applying invasive BMI procedures to severely paralyzed patients.